SMiRT-12 / K. Kussmaul (Editor)

GF09/4

FRACTURE PROPERTIES EVALUATION OF BOP PIPING SYSTEMS FOR THE YONGGWANG 3&4 NUCLEAR GENERATING STATION

Y.J. Kim[1], Y.S. Choy[1], C.S. Seok[1], K.M. Yang[2], I.A. Ra[2] and H.Y. Ahn[3]

[1]Sung Kyun Kwan University, Suwon, Korea
[2]Korea Power Engineering Company, Seoul, Korea
[3]Korea Heavy Industry and Construction Co., Changwon, Korea

1 INTRODUCTION

In order to apply a leak-before-break(LBB) design concept to nuclear piping system, a technical report which demonstrates the stability of piping system has to be prepared. The stability assessment of piping system is based on the material properties of the archival piping materials.

A comprehensive material test program was prepared to generate material properties as required for the LBB application to the Yonggwang 3&4 balance of plant(BOP) piping system(Yang et al, 1993). A total of 125 tensile tests was performed to determine their stress-strain behaviour, and a total of 93 fracture toughness tests was performed to determine their J-resistance behaviour. In this paper, the LBB material test program on the Yonggwang BOP piping system is described and the effects of various factors on the material properties are discussed.

2 MATERIAL TEST PROGRAM

2.1 Test Methodlogy

According to the NUREG-1061 Vol.3(USNRC, 1984), at least two stress-strain curves and two J-resistance curves should be developed for each of a minimum of three heats of materials having the same material specifications and thermal and fabrication histories as the in-service piping material. If the data are being developed from an archival heat of material, a minimum of three stress-strain curves and three J-resistance curves from that one heat of material is sufficient. In order to develope LBB material properties for the Yonggwang BOP piping systems, the following steps were taken.

Step 1: Perform impact tests and select three heat numbers having the lowest impact energy.

Step 2: Perform upper temperature tensile tests(L and C orientations) for the selected heat numbers.

Step 3: Perform upper temperature fracture toughness tests(L-C and C-L orientations) for the selected heat numbers.

Step 4: Select the heat number having the lowest fracture energy among the upper temperature fracture toughness test results(L-C orientation), and perform low temperature tensile tests(L orientation) and low temperature fracture toughness tests(L-C orientation)

Step 5: Select three heat numbers having median strength values for each piping, and perform two upper temperature tensile tests(L and C orientations) for each heat number.

Fig.1 shows the specimen orientation with suspect to a pipe geometry.

2.2 Test Material

Test materials were SA312 TP316, SA312 TP304, SA106 Gr.C and associated welds. Weld materials were prepared by shop and field fabrications using full gas tungsten arc welding(GTAW) procedure. Table 1 summurizes the test material, pipe diameter, thickness, required number of specimens and test temperature.

The test specimens for SA312 TP316 stainless steel were machined from the 12", 14", 16" pipes, and the test specimens for SA312 TP304 stainless steel were machined from the 14" pipe. The test specimens for SA106 Gr.C carbon steel were machined from the 26 3/8", 26 5/8" pipe and the 26 5/8" elbow.

2.3 Test Specimen

For SA106 Gr.C steel and SA312 TP316 steel, 1/2"ϕ round bar specimens were used for tensile tests and 1T-CT(compact tension) specimens were used for fracture toughness tests. However for relatively thin SA312 TP304 steel, the largest specimens that could be machined were used.

2.4 Test Method

Tensile tests were performed in accordance with ASTM E8(Standard Test Methods of Tension Testing of Metallic Material) and E21(Standard Recommended Practice for Elevated Temperature Tension Tests of Metallic Materials). Upper temperature tests were performed after maintaining the required temperature for two hours. The 0.2% offset method was adopted to determine the yield strength values except for the case of SA106 Gr.C steel tests at low temperature.

Fracture toughness tests were performed in accordance with ASTM E813(Standard Test Methods for J_{IC}, A Measure of Fracture Toughness) and E1152(Standard Test Method for Determining J-R Curves). An unloading compliance technique with high temperature COD gage was utilized to determine the J-R curves.

3 Test Results and Discussions

In this section, test results are grouped and summerized to show the effect of various factors which have an influence on the fracture properties. Discussion will be focused on the carbon steel data.

Table 1 Yonggwang BOP LBB Test Program Summary

Material		Size	σ-ε Test		J-R Test		Temp. (℃)	
			Upper	Lower	Upper	Lower	Upper	Lower
Base Metal	SA312 TP316	12" S/160	12	1	4	1	49	20
		14" S/160	12		4		296	
		16" S/160	12		4		327	
	SA312 TP304	14" S/STD	12	1	12	1	49	
	SA106 Gr.C (Pipe)	24.047" x1.046"t	10	1	6	1	296	121
	SA106 Gr.C (Elbow)	24.047" x1.046"t	8	1	8	1		
	SA106 Gr.C (Pipe)	24.047" x1.627"t	10	1	6	1		
Shop Fab. Weld Metal	SA312 TP316	12" S/160	3	1	3	1	49	20
		14" S/160	3	1	3	1	296	
		16" S/160	3	1	3	1	327	
	SA312 TP304	14" S/STD	3	1	3	1	49	
	SA106 Gr.C (Pipe)	24.047" x1.046"t	3	1	3	1	296	121
Field Fab. Weld Metal	SA312 TP316	12" S/160	3	1	3	1	49	20
		14" S/160	3	1	3	1	296	
		16" S/160	3	1	3	1	327	
	SA312 TP304	14" S/STD	3	1	3	1	49	
	SA106 Gr.C (Pipe)	24.047" x1.046"t	3	1	3	1	296	121
	SA106 Gr.C (Pipe)	24.047" x1.046"t	3	1	3	1		

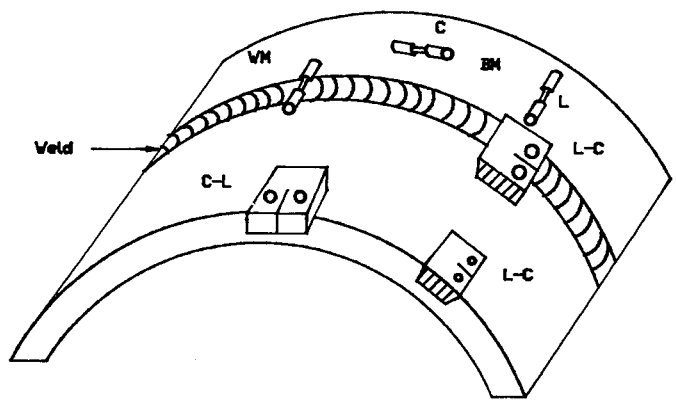

Fig.1 Specimen orientation with respect to a pipe geometry

3.1 Test Results

For tensile tests, the nominal stress-strain curves were obtained from the load-displacement curves and the yield strength and tensile strength values were determined. Subsequently the true stress-strain curves were generated and, by curve-fitting to the Ramberg-Osgood equation, α, n material constants were obtained.

For fracture toughness tests, J-R curves were obtained from the load versus load line displacement curves. Accordingly C_1, C_2 and J_{IC} values were then obtained by a power law curve fitting method. The ASTM validity requirements such as data spacing, reglession line, crack shape and amount of crack extension were satisfied. However the ASTM requirements for J_{MAX} and ω were not satisfied. This may be due to the high toughness values of the tested materials.

3.2 Effect of Product Form

Fig.2 shows the upper temperature tensile test results for SA106 Gr.C steel in L orientation. Although the stress-strain curves of 26" and 27" pipes were similar, the stress-strain curves of 26" elbow were lower than those of 26" pipe. Similar trends were also observed for both upper temperature stress-strain curves in C orientation and lower temperature stress-strain curves in L orientation.

Fig.3 shows the upper temperature fracture toughness test results for SA106 Gr.C steel in C-L orientation. Against the tensile test results, the J-resistance of 26" elbow was higher than that of 26" pipe. Similar phenomena were also observed for both upper and lower temperature J-resistance curves in L-C orientation.

3.3 Effect of Crack Plane Orientation

Fig.4 shows the upper temperature fracture toughness test results for SA106 Gr.C steel. This figure shows that the fracture toughness in L-C orientation is higher than that in C-L orientation. The variation of toughness with orientation is related to the principal direction of mechanical working or grain flow in pipes and forgings. Similar material behavior in carbon steel piping has been observed by other investigator(Mukherjee, 1988). However, this effect was not significant for SA312 TP316 steel.

3.4 Effect of Temperature

Fig.5 shows the effect of temperature on fracture toughness for SA106 Gr.C steel. This figure shows that the J-resistance curves for base metals at 289℃ are lower than those at 121℃. Examination of the load versus load line displacement results recorded during the fracture toughness tests exhibited evidence of strain aging. Similar phenomenon was also observed in carbon steel data of SA106B(Mukherjee, 1988) and SA516-70(Kim and Prince, 1987).

3.5 Effect of Welding

Fig.6 shows the effect of welding on stress-strain curves for SA106 Gr.C steel. Although the stress-strain curves of the weld metal are higher than those of the base metal, it was not possible to obtain full stress-strain curves for weld metal specimens due to the necking of the region outside of the gage length. Similar phenomena were also observed in SA312 TP316 steel.

Fig.7 shows the effect of welding on J-resistance curves. As shown in the figure, the J-resistance curves of the weld metal were higher than those of the base metal. Also the J-resistance curves of the weld metal fabricated by the field welding procedure were higher than those of the weld metal fabricated by the shop welding proceure.

4 CONCLUSION

Following conclusions were made from the LBB material test program on the Yonggwang 3&4 BOP piping materials.

1) Material properties of weld metal were in general higher than those of base metal.
2) Fracture toughness values in L-C orientation were higher than those in C-L orientation.
3) Fracture toughness values at upper temperature range were lower than those at lower tempeature.
4) Due to the high ductility of the piping material, the ASTM specimen size requirement was not satisfied.

Reference

Kim,Y.J. and Prince,J.W. (1987). Temper-Bead Weld Heat-Affected Zone Properties in A516-70 Steel, ASME Journal of Engineering Materials and Technology, Vol.109, pp.157-163.

Mukherjee,B. (1988). The J-Resistance Curve Leak-Before-Break Test Program on Material for the Darlington Nuclear Generating Station, Int.J. of Pressure Vessel and Piping, Vol.31, pp.363-385.

Yang,K.M., Ra,I.S., Kim,Y.J. and Field,R.M. (1993). Leak Before Break Evaluation of BOP Piping System for The Yonggwang 3&4 Nuclear Generating Sation, To be presented at the 12th SMIRT Conference.

USNRC. (1984). Evaluation of Potential for Pipe Breaks, NUREG-1061 Vol.3.

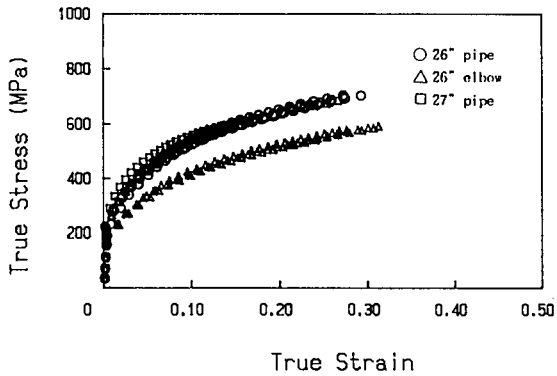

Fig. 2 Effect of product form on σ-ε curves(SA106 Gr.C)

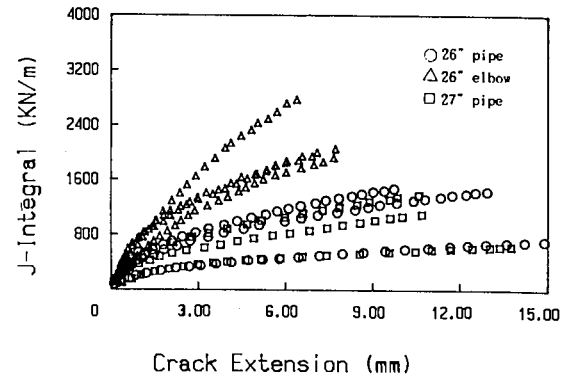

Fig. 3 Effect of product form on J-R curves (SA106 Gr.C)

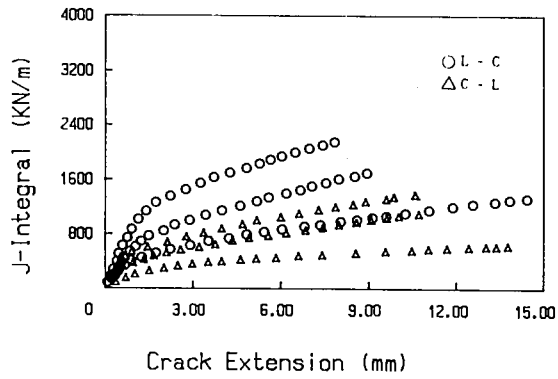

Fig. 4 Effect of orientation on J-R curves(SA106 Gr.C)

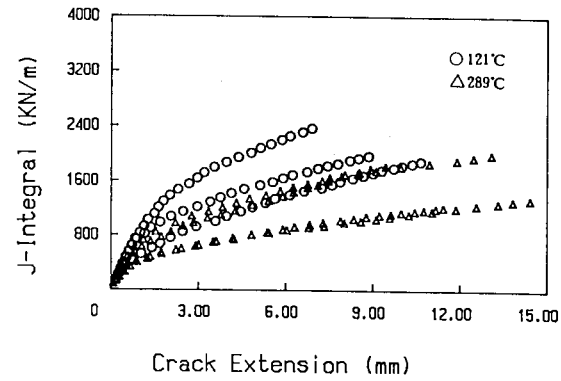

Fig. 5 Effect of test temperature on J-R curves(SA106 Gr.C)

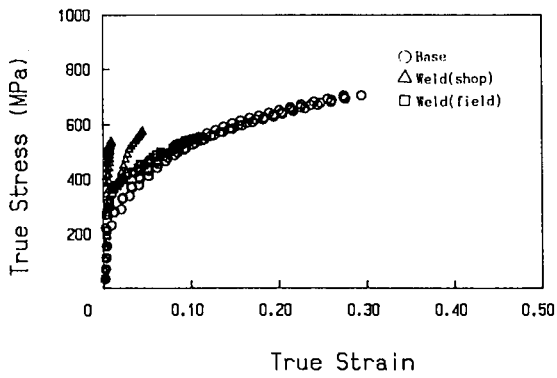

Fig. 6 Effect of welding on σ-ε curves(SA106 Gr.C)

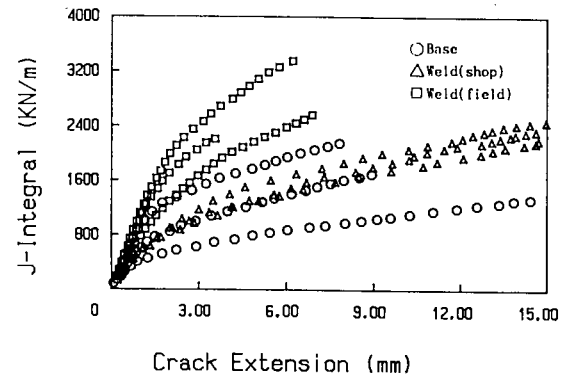

Fig. 7 Effect of welding on J-R curves (SA106 Gr.C)